Determining the self-inductance profile of switched reluctance motors using a recursive Fourier algorithm

A.C. Oliveira[1,2], C.B. Jacobina[1] e A.M.N. Lima[1]
[1] Universidade Federal da Paraíba
UFPB/CCT/DEE/LEIAM - Campus II - Caixa Postal 10105
58.109-970 Campina Grande, PB, Brazil.
Fax: +55-83-3101015
[2] Centro Federal de Educação Tecnológica do Maranhão - CEFET-MA
{aco,jacobina,amnlima}@dee.ufpb.br

Abstract **- This article proposes a technique for determining the self-inductance of a switched reluctance machine. In the proposed technique the stator phase windings are supplied with a sinusoidal voltage source of constant frequency and constant amplitude while the shaft rotates driven externally. In this case the phase current is amplitude modulated due to the variation of the self-inductance with the shaft position. A recursive Fourier algorithm is employed to extract the inductance profile from the envelop of the phase current. The mathematical formulation of the technique proposed and its application for a 6/4 (three-phase) switched reluctance machine are presented.**

I. Introduction

The technological advances of the last decades made possible the practical use of the switched reluctance motors. This type of motor presents magnetic saliences in both rotor and stator and require an electronic circuitry to provide the commutation synchronized with the shaft position.

The knowledge of the profile of the self-inductance of the phase versus shaft position $L(\theta)$ as well as its derivative with respect to the position $dL(\theta)/d\theta$ are very important information for controlling a switched reluctance motor. Indeed, the profile of the self-inductance defines the commutation angles while its derivative allows to design the current waveform that provides smooth electromagnetic torque [1, 2]. The design of the current waveform for smooth torque and the determination of the correct commutation angles are critical issues for variable speed drive systems with switched reluctance motors.

There are several techniques for determining the inductance profile of a switched reluctance motor. One of the most common techniques consists in mechanically positioning the shaft at a given angle, supply the stator windings with a step voltage waveform and record the phase current. The inductance at that position can be determined either from the rise time of the stator current waveform or from the slope of the flux linkage versus current characteristic curve. The very basic disadvantage of these type of techniques is the need of mechanically positioning the shaft at various different angular positions to obtain the complete self-inductance profile. Besides, that it is required to lock the shaft at every position to avoid the natural alignment toward to the maximum inductance position when the phase is energized to record the current. The positioning and locking of the shaft of the switched reluctance motor such that an entire cycle of the inductance profile be visited with reasonable and accurate angular steps requires the utilization of a servomotor drive. The use of a servomotor increases quite significantly the cost of the characterization platform.

This article proposes a technique that does not require the locking of the shaft at different positions of the entire cycle of the inductance profile. In the proposed technique the stator windings are supplied with a sinusoidal voltage source of constant frequency and constant amplitude while the shaft freely rotates driven externally. The inductance profile is determined from the envelop of the phase current waveform that is amplitude modulated. The envelop is extracted by using a recursive Fourier algorithm [3].

II. Switched reluctance motor

Figure 1 shows the electromagnetic structure of a six stator poles and four rotor poles (6/4) switched reluctance motor. Both the stator and the rotor have strong magnetic saliencies. The rotor cores are made by stacking laminations that have been punched from magnetic quality lamination steel. There are no windings, die castings or commutator to contend with. The stator also is formed from punched laminations that have been bonded into a core. The number of stator poles is different from the number of rotor poles in order to provide good starting performance. The six windings of the stator are grouped in pairs for each phase. In this case the windings are connected in series and consequently for the configuration shown in the figure there are six poles but only three-phases. The most common electromagnetic structures of switched reluctance motors are: 4/2 (two phases), 6/4 (six phases), 6/8 (six phases), 8/6 (four phases), 10/8 (five phases) e 12/8 (three phases) [4].

A. Motor model

The state space representation for a switched reluctance motor is given by

$$\frac{d}{dt}\lambda_k(\theta, i) = v_k - r_k i_k \qquad (1)$$

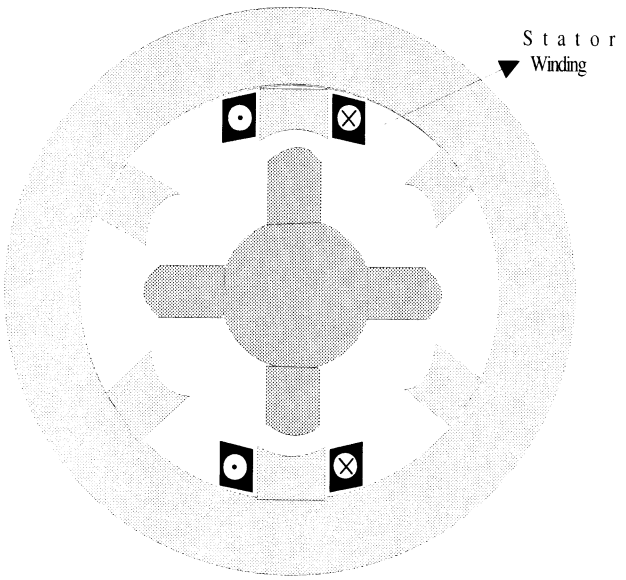

Fig. 1 Electromagnetic structure of a 6/4 switched reluctance motor: six stator poles and four rotor poles.

$$\frac{d}{dt}\omega = -\frac{F}{J}\omega + \frac{1}{J}(\tau_e - \tau_l) \quad (2)$$

$$\frac{d}{dt}\theta = \omega \quad (3)$$

where:

v_k voltage applied to the k^{th} stator winding (V)
i_k current flowing through k^{th} stator winding (A)
$\lambda_k(\theta, i)$ total flux linkage for the k^{th} windings (Wb)
r_k stator resistance of the k^{th} winding (Ohm)
ω angular speed (rad/s)
θ angular positions (rad)
τ_e electromagnetic torque (Nm)
τ_l load torque (Nm)

The total flux linkage for the k^{th} phase can be calculated by

$$\lambda_k(\theta, i) = \sum_{n=1}^{N} L_{kn}(\theta, i_n) i_n \quad (4)$$

where N is the number of the stator phases and $L_{kn}(\theta, i_n)$ is the mutual inductance from phase k to phase n. However, it is usual to consider that $L_{kn}(\theta, i_n)$, $k \neq n$ is negligible [4] and in this case equation (4) becomes

$$\lambda_k(\theta, i) = L_k(\theta, i_k) i_k \quad (5)$$

and consequently the first equation of the state space model can be rewritten as

$$v_k = r_k i_k + L_k(\theta, i_k)\frac{di_k}{dt} + i_k \frac{\partial L_k(\theta, i_k)}{\partial i_k}\frac{di_k}{dt} + \omega i_k \frac{\partial L_k(\theta, i_k)}{\partial \theta} \quad (6)$$

The electromagnetic torque of the switched reluctance motor can be calculated from the co-energy as

$$\tau_e = \frac{\partial}{\partial \theta}\int L_k(\theta, i_k) i_k di_k \quad (7)$$

If magnetic saturation is neglected, the phase inductance will no longer depend on the phase current and consequently the equation (7) becomes

$$\tau_e = \frac{1}{2} i_k^2 \frac{dL_k(\theta)}{d\theta} \quad (8)$$

Equation (8) shows a relevant feature of this type of motor, namely the fact that the electromagnetic torque is proportional to the square of the phase currents and consequently is independent of the polarity of the phase current. Then a power converter designed to supply a switched reluctance motor must provide only unidirectional currents.

The simplest way to supply the switched reluctance motor is to energize the phase when $dL(\theta)/d\theta$ becomes positive and de-energize when $dL(\theta)/d\theta$ becomes negative. Then the commutation process is provided electronically and is synchronized with the angular shaft position.

B. Phase current envelop

Lets consider that the stator winding of a switched reluctance motor are fed with a sinusoidal voltage source. If the frequency of this voltage excitation waveform is constant and sufficiently high it is possible to neglect the resistive voltage drop and then equation (1) can be simplified to

$$v_k \approx \frac{d\lambda_k(\theta, i)}{dt}. \quad (9)$$

In sinusoidal steady-state, neglecting the couplings between phases, as usual,

$$V_k = j\omega_c L_k(\theta) I_k \quad (10)$$

and consequently

$$I_k = \frac{V_k}{j\omega_c L_k(\theta)} \quad (11)$$

Note that according to (11) if the amplitude of the stator voltage is kept constant, then the stator current amplitude is modulated due to the variation of the self-inductance $L_k(\theta)$. Then, detecting the amplitude of fundamental component of the stator current we can determine the reactance of the phase, i.e.,

$$X_{L_k}(\theta) = \frac{V_k}{I_k(\theta)} \quad (12)$$

where V_k is the amplitude of stator voltage supplied to the k^{th} phase and $I_k(\theta)$ is the amplitude of the fundamental component of the stator current that is obviously dependent on the instantaneous shaft position. The determination of the phase inductance is straightforward

$$L_k(\theta) = \frac{X_{L_k}(\theta)}{2\pi f_c} \quad (13)$$

where f_c is the frequency of the stator voltage source. It is also assumed that the shaft position does not change significantly during a cycle of the exciting voltage.

The amplitude of fundamental component of the phase current can be determined by using the recursive Fourier algorithm described in the following section.

III. Recursive Fourier algorithm

The complete cycle Fourier algorithm was proposed in [5] to determine the amplitude and phase of a signal from its uniformly sampled measurements

$$\{y(1), y(2), \cdots, y(N_p)\}.$$

For this algorithm it is assumed that the measurements can be represented by

$$y(t) = B\sin(\omega_o t\Delta\tau + \delta_o) \tag{14}$$

or equivalently

$$y(t) = B_c\cos(\omega_o t\Delta\tau) + B_s\sin(\omega_o t\Delta\tau)$$

where $t = 1, 2, ..., N_p$, $\Delta\tau$ is the sampling interval, N_p is the number of samples period, $B_c = B\cos(\delta_o)$ and $B_s = B\sin(\delta_o)$. Given B_c and B_s the values of B and δ_o can be calculated by

$$B = \sqrt{B_c^2 + B_s^2}, \tag{15}$$

$$\delta_o = \arctan\left(\frac{B_c}{B_s}\right). \tag{16}$$

The Fourier analysis of a given signal is an extension of the equation (14) where more harmonics are included. For every harmonic term, the amplitudes B_c and B_s can be determined by using

$$B_c = \frac{2}{N_p}\sum_{t=1}^{N_p} y(t)\cos\left(\frac{2\pi mt}{N_p}\right) \tag{17}$$

$$B_s = \frac{2}{N_p}\sum_{t=1}^{N_p} y(t)\sin\left(\frac{2\pi mt}{N_p}\right) \tag{18}$$

where $m = 1, 2, , \cdots$ represent the order of the harmonic term.

If $m = 1$, the use of (17)-(18) and (15)-(16) provides the phase and the amplitude of the measured signal. These equations are in the batch format, i.e., N_p samples are required before the result can be calculated.

However, the use of a sliding window allows one to rewrite these equations in a recursive format, i.e., a result can be provided at every new sampled measurement. The derivation of the recursive version will be presented only for the term B_c since it can be adapted easily for a the term B_s. Consider a sliding window with N_p samples and $t \leq N_p$ then

$$B_c(t) = \frac{2}{N_p}\sum_{k=1}^{t} y(k)\cos\left(\frac{2\pi mk}{N_p}\right) \tag{19}$$

but for $t - 1 \leq N_p$ similarly

$$B_c(t-1) = \frac{2}{N_p}\sum_{k=1}^{t-1} y(k)\cos\left(\frac{2\pi mk}{N_p}\right) \tag{20}$$

If $t > N_p$ this means that an entire cycle of data has been collected. Then to keep a sliding window with N_p samples the term $B_c(t - N_p)$ must be discarded from the sum given in (19), i.e.,

$$\begin{aligned} B_c(t) &= B_c(t-1) + \frac{2}{N_p}y(t)\cos\left(\frac{2\pi mt}{N_p}\right) \\ &\quad -\frac{2}{N_p}y(t-N_p)\cos\left(\frac{2\pi m(t-N_p)}{N_p}\right) \end{aligned} \tag{21}$$

But for a complete cycle we have that

$$\cos\left(\frac{2\pi m(t-N_p)}{N_p}\right) = \cos\left(\frac{2\pi mt}{N_p}\right) \tag{22}$$

whereas for a half cycle

$$\cos\left(\frac{\pi m(t-N_p)}{N_p}\right) = -\cos\left(\frac{\pi mt}{N_p}\right). \tag{23}$$

Using these identities we obtain the recursive complete cycle discrete Fourier algorithm given by

$$\begin{aligned} B_c(t) &= B_c(t-1) + \frac{2}{N_p}y(t)\cos\left(\frac{2\pi mt}{N_p}\right) \\ &\quad -\frac{2}{N_p}y(t-N_p)\cos\left(\frac{2\pi mt}{N_p}\right) \end{aligned} \tag{24}$$

$$\begin{aligned} B_s(t) &= B_s(t-1) + \frac{2}{N_p}y(t)\sin\left(\frac{2\pi mt}{N_p}\right) \\ &\quad -\frac{2}{N_p}y(t-N_p)\sin\left(\frac{2\pi mt}{N_p}\right) \end{aligned} \tag{25}$$

IV. Experimental results

The proposed technique was implemented in the laboratory using the experimental platform shown in Fig. 2. As shown in the diagram, the phase winding is supplied with a voltage source provided at the output of a push-pull power amplifier represented by Block A. For the tests presented in this article, the phase to be excited by this voltage source is selected manually with help of the switch CH. However, the automation of this process is quite simple. For each phase, the current waveform was recorded for a full turn of the motor shaft in order to detect possible asymmetries of the inductance profile. The voltage of the excited phase and the induced voltages of the other phases were measured through LV25-P transducers represented by the several Blocks V. The phase current was measured through the LA25-NP transducer represented by Block I. The sinusoidal signal with frequency of 100Hz and amplitude of 3V was obtained from an HP signal generator (V_i) . All the measured voltage and current signals were acquired through 12-bit analog to digital converters of a dedicated plug-in board installed in a PC slot.

In the test platform, the switched reluctance motor is mechanically coupled to a DC motor and to a 9-bit gray code position encoder. For the tests presented in this article, the shaft speed was defined by the DC motor. However, the use of any mechanical means for providing a full rotation of the shaft of the switched reluctance motor

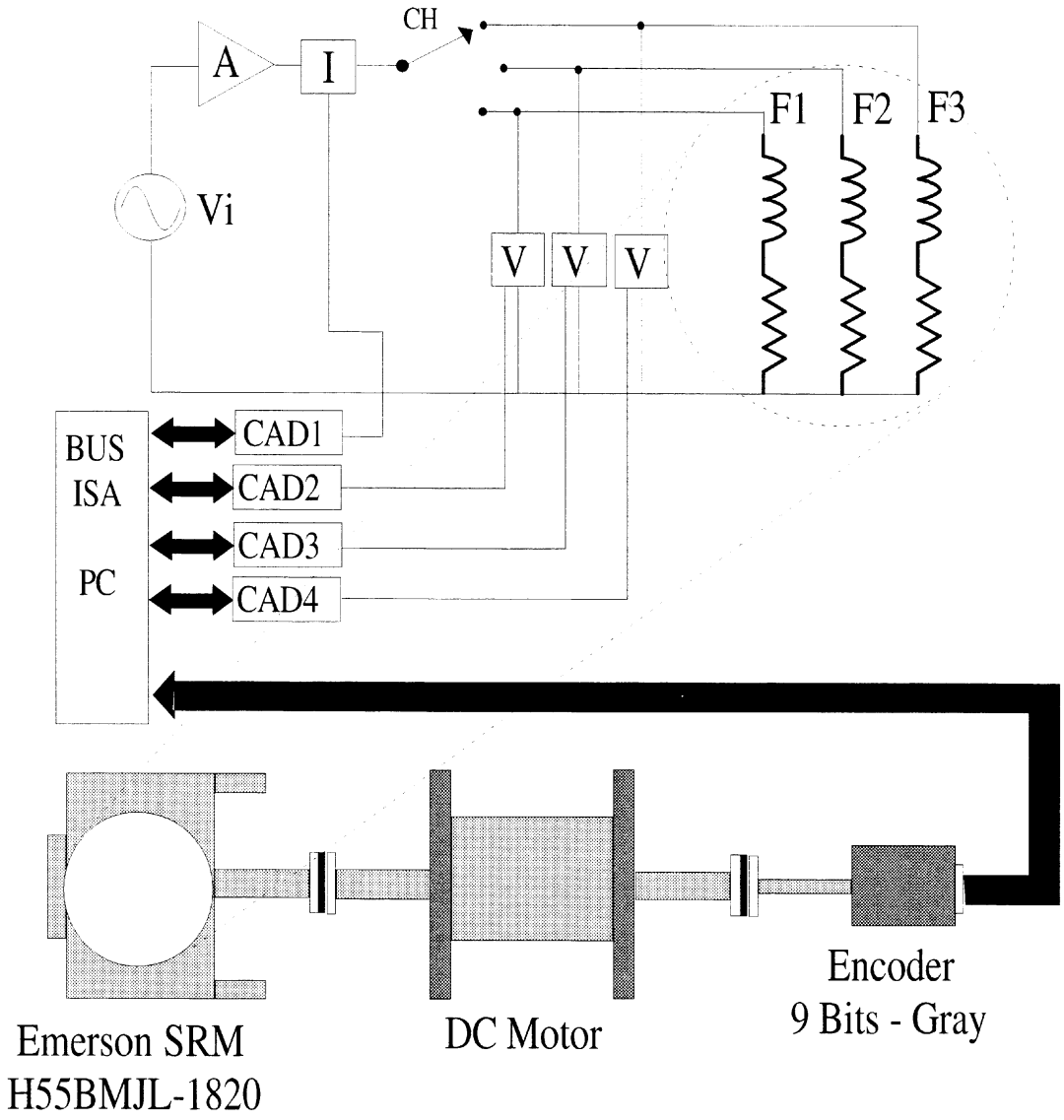

Fig. 2 Simplified diagram of the platform used in the experimental tests.

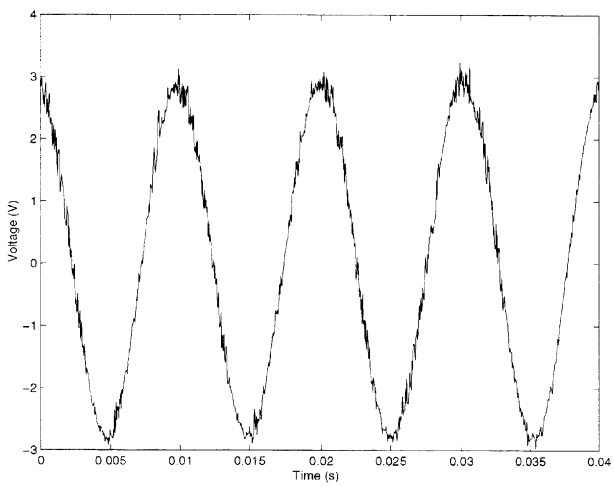

Fig. 3 Voltage waveform applied to the stator phases.

can also be employed. The phase current measured under these conditions is shown in Fig. 4. This figure shows clearly the amplitude modulation due to the variation of the inductance with the angular position. It is also important to remark that the average value of the phase current is zero and consequently the motor does develop any electromagnetic torque and the shaft could even be rotated manually without any difficulty.

The envelops of the voltage and current waveforms were determined by using the recursive Fourier algorithm. Figures 5 and 6 show the results obtained for $N_p = 250$ points and $\Delta\tau = 40\mu s$. The amplitude of voltage applied to the stator phases is nearly constant and consequently the modulation observed in the phase currents is only due to the self-inductance variation.

Figure 7 shows the self-inductance profiles of the phases of the 6/4 motor used in the experimental tests. Several tests were repeated for different amplitudes and frequencies but not shown here due to space limitations. Some of

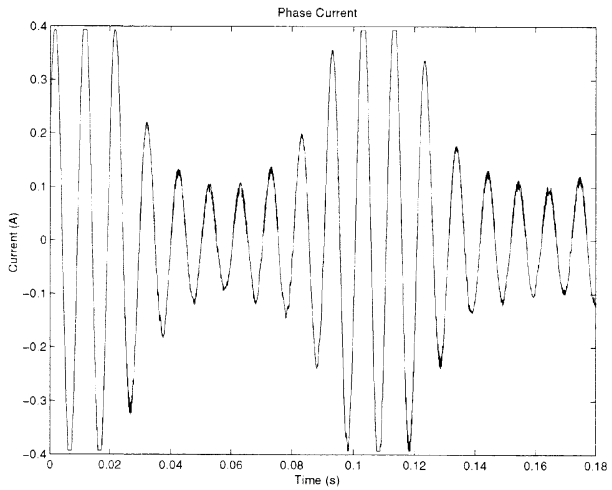

Fig. 4 Phase current of the switched reluctance motor.

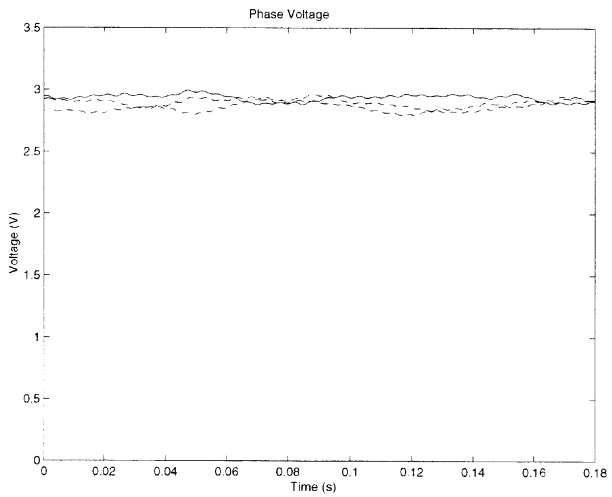

Fig. 5 Envelop of the phase voltage applied to the stator phases.

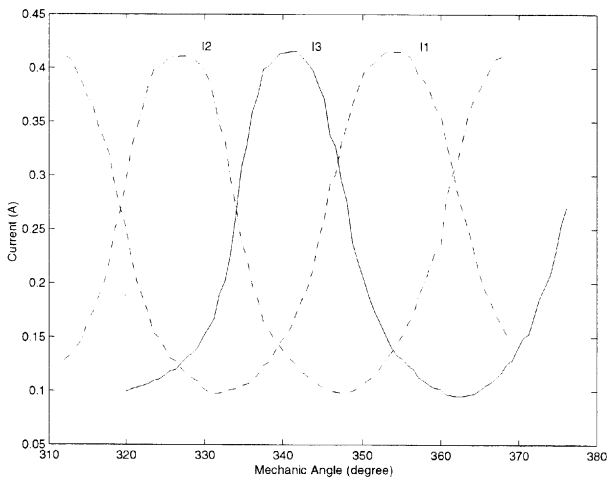

Fig. 6 Envelop of the phase currents as obtained with the recursive Fourier algorithm.

these tests revealed a limitation with respect to the maximum frequency of the voltage excitation. If the frequency is increased severe distortions appears in the phase currents. This can be attributed to the frequency response of the ferromagnetic material used to construct the motor. The formulation presented in this article was based on the assumption that the resistive voltage drop can be neglected. However, if the frequency of stator voltage source does not allows this approximation it is necessary to include the resistive term in the reactance expression provided a reasonable estimate of the stator resistance is known, i.e.,

$$L_k(\theta) = \frac{\sqrt{(X_{L_k}(\theta)^2 - r_k^2)}}{2\pi f_c} \tag{26}$$

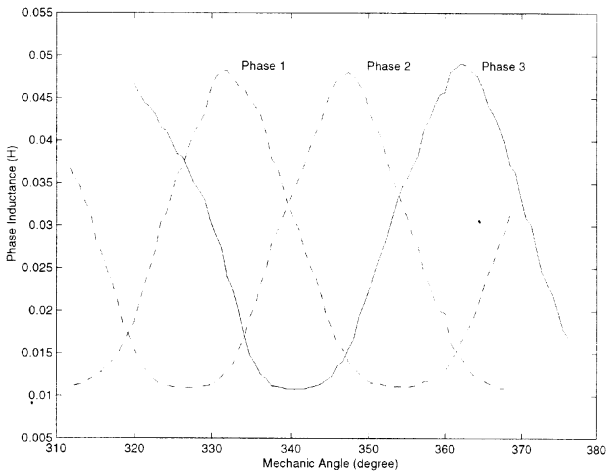

Fig. 7 Profile of the self-inductance of the 6/4 motor as obtained with the proposed technique.

In order to access the usefulness of the proposed technique we have also determined the self-inductance profile by using the so-called classical technique to compare its results. In the classical technique the self-inductance profile is determined from the relationship between the flux linkage versus current at a given angular position for a step voltage applied to the phase winding.

Figures 8 and 9 show the waveforms of current versus time and flux linkage versus current as obtained from the classical technique, respectively. The experimental platform used in the previous tests was adapted to implement the classical technique. However, note that in Figs. 8 and 9 the angular step is not uniform due to the difficult of positioning the shaft without a servomotor. Figure 8 shows that the rise time increases as the rotor moves to the alignment position where the self-inductance is maximum. The step voltage of 10V applied to the phase during this test was removed when the phase current attained 3.5A. Figure 9 shows that there is a linear relationship between the flux linkage and the phase current indicating that the magnetic saturation is not observed for motor currents below 3.5A.

Figure 10 shows the self-inductance profile as obtained from the classical technique. In fact this curve is obtained

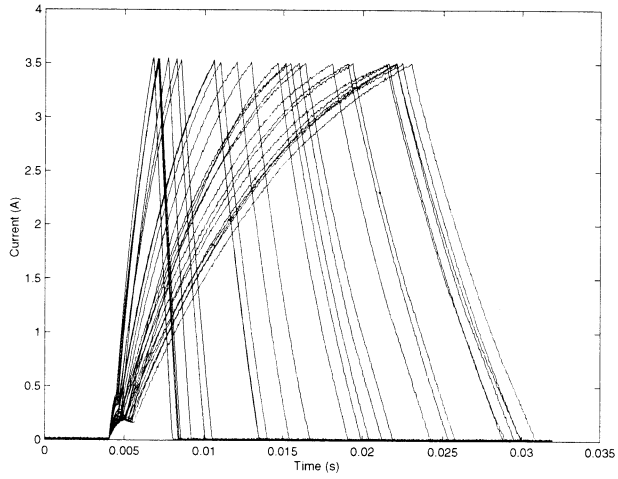

Fig. 8 Phase current versus time

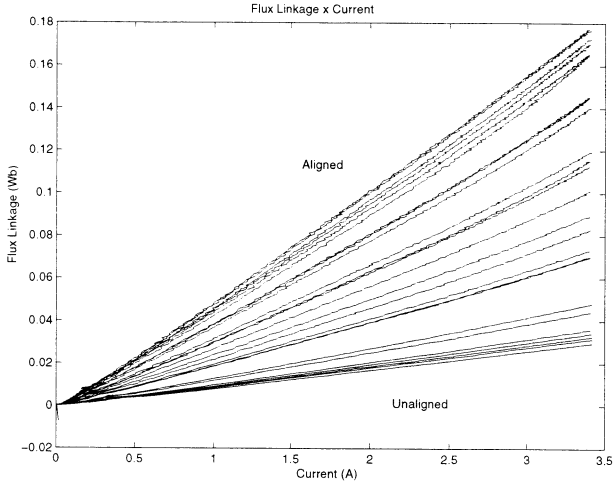

Fig. 9 Flux linkage versus current

by calculating the slope of the flux linkage versus current at a specific angular position.

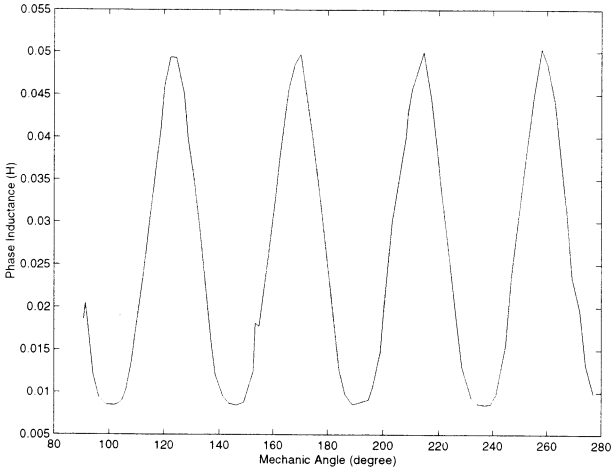

Fig. 10 Self-inductance profile as obtained with the classical technique.

V. Conclusion

This article shows how to estimate the self-inductance profile of a switched reluctance motor by using recursive Fourier analysis of the phase current waveform when the stator windings is supplied with a sinusoidal voltage source. The technique proposed is relatively simple and does not require neither to lock the shaft at specific positions nor computing the slope of the flux linkage versus current. For the 6/4 motor available in the laboratory, we have used 100Hz for frequency of the stator voltage source. The self-inductance profile obtained with the technique proposed has shown a reasonable agreement with the results obtained with the classical technique that was also implemented in the laboratory.

For the proposed technique it is not required to have a precise control of the shaft speed. Indeed, the shaft can even vary during the experiment. However, the speed must be slow enough to make sure that the shaft position be essentially constant for a full cycle of the frequency of the stator voltage source. For the tested motor excited with a sinusoidal of 100Hz the speed of 12rpm that provided a variation of 0.72 degrees for a cycle of 10ms (100Hz) was a good choice.

Acknowledgments

The authors thank CNPq (Conselho Nacional de Desenvolvimento Científico e Tecnológico), CAPES (Fundação Coordenação de Aperfeiçoamento de Pessoal de Nível Superior) for the award of research and study fellowship during the course of these investigations and Emerson Motor Company for providing the switched reluctance motor used in the laboratory experiments.

REFERENCES

[1] Nicholas J. Nagel. *Complex Rotating Vector Analysis and Control of a Switched Reluctance Motor.* PhD thesis, University of Wisconsin - Madison, 1998.

[2] I. Husain and M. Ehsani. Torque ripple minimization in switched reluctance motor drives by pwm current controle. *IEEE Transactions on Power Electronics*, 11(1):83–88, 1996.

[3] L.A.L. Almeida T.M. Oliveira, A.C. Oliveira and C.B. Jacobina. Algoritmo robusto para sincronização de sistemas em acionamento de máquinas. In *Conf. Rec. CBA*, pages 1509–1514, 2000.

[4] T. J. E. Miller. Switched reluctance motors and their control. In *Magna Physics Publishing and Clarendon Press*, 1993.

[5] M. Ramamoorty. Application of digital computers to power system protection. *Jornal of Inst. Eng.*, 52(10):235–238, 1972.